7998 *Biochemistry* **2010,** *49,* 7998–8005
DOI: 10.1021/bi100962h

BIOCHEMISTRY
including biophysical chemistry & molecular biology
Article

NMR Studies of Translocation of the Zif268 Protein between Its Target DNA Sites[†]

Yuki Takayama, Debashish Sahu, and Junji Iwahara*

Department of Biochemistry and Molecular Biology, Sealy Center for Structural Biology and Molecular Biophysics, University of Texas Medical Branch, Galveston, Texas 77555-1068

Received June 14, 2010; Revised Manuscript Received August 17, 2010

ABSTRACT: Zif268 is a zinc-finger protein containing three Cys_2-His_2-type zinc-finger domains that bind the target DNA sequence GCGTGGGCG in a cooperative manner. In this work, we characterized translocation of the Zif268 protein between its target DNA sites using NMR spectroscopy. The residual dipolar coupling data and NMR chemical shift data suggested that the structure of the sequence-specific complex between Zif268 and its target DNA in solution is the same as the crystal structure. Using two-dimensional heteronuclear $^{1}H-^{15}N$ correlation spectra recorded with the fast acquisition method, we analyzed the kinetics of the process in which the Zif268 protein transfers from a target site to another on a different DNA molecule on a minute to hour time scale. By globally fitting the time−course data collected at some different DNA concentrations, we determined the dissociation rate constant for the specific complex and the second-order rate constant for direct transfer of Zif268 from one target site to another. Interestingly, direct transfer of the Zif268 protein between its target sites is >30000-fold slower than corresponding direct transfers of the HoxD9 and the Oct-1 proteins, although the affinities of the three proteins to their target DNA sites are comparable. We also analyzed translocation of the Zif268 protein between two target sites on the same DNA molecules. The populations of the proteins bound to the target sites were found to depend on locations and orientations of the target sites.

Most transcription factors recognize particular DNA sequences (target sites) and bind to them with high affinities. Structural biology has provided an enormous amount of the structural information on sequence-specific protein−DNA interactions. Currently, the Protein Data Bank contains the three-dimensional structures of more than 1500 protein−DNA complexes. Compared to the wealth of structural information, biophysical knowledge of the other aspects of the protein−DNA interactions remains relatively poor. Although NMR[1] spectroscopy can provide information about the dynamic and kinetic aspects of macromolecular interactions in solution, most NMR studies on protein−DNA interactions have focused on their structural aspects (e.g., reviewed in refs *1* and *2*). It is relatively recent that NMR investigations on the dynamic process whereby DNA-binding proteins find their target sites were initiated (*3*−*9*). This field is still in an early stage of advancement, and there is considerable room for further methodological development.

In this work, we demonstrate unique NMR approaches to characterize relatively slow translocation of proteins between their target DNA sites, which cannot be analyzed by the approaches used in previous studies. We applied the new NMR approach to the investigation of the Zif268 (also known as Egr-1) protein. Zif268 is an inducible transcription factor that acts as a messenger coupling neurotransmission to a cascade of altered gene expression for neuronal plasticity and memory formation (*10*−*15*). Zif268 contains three Cys_2-His_2-type zinc-finger domains (*16*) that cooperatively bind the target DNA sequence GCGTGGGCG as a monomer (Figure 1a). In this paper, "the Zif268 protein" refers to a protein construct containing the three zinc-finger domains (Zif268 residues 335−423). The sequence specificity and binding affinity of the Zif268 protein to DNA have been well studied (*17*−*27*), and crystal structures have been determined for Zif268/DNA complexes as well as for the complexes of the engineered Zif268 mutant proteins with their target DNA (*22*, *28*−*33*). In the present work, we have studied translocation of the Zif268 protein between its target DNA sites.

MATERIALS AND METHODS

Protein Preparation. The gene encoding the zinc-finger regions of human Zif268 (residues 335−432) was made from chemically synthesized DNA oligonucleotides and amplified by PCR. The codons in the synthetic gene were optimized for optimal gene expression in *Escherichia coli*. The gene was inserted into the pET-49b vector (Novagen). *E. coli* strain BL21(DE3) harboring the resultant plasmid was cultured in 4 L of minimal media for expression of a glutathione *S*-transferase (GST)−Zif268 fusion protein. [^{13}C]Glucose and [^{15}N]ammonium chloride were used for isotope labeling of the protein. At OD_{600} = 1.0−1.2, the protein expression was induced by the addition of 0.2 mM isopropyl β-D-1-thiogalactopyranoside, and 50 μM $ZnCl_2$ was added to the media. After the induction, the culture temperature was lowered from 37 to 24 °C, and cells were cultivated for further 18 h. Cells were harvested by centrifugation at 4000*g* and suspended in ∼100 mL of buffer containing 50 mM Tris-HCl (pH 7.5), 500 mM NaCl, 5% glycerol, 1% Triton X-100, and 2 tablets of the EDTA-free protease inhibitor cocktail (Roche).

[†]This work was supported by Grant MCB-0920238 from the National Science Foundation and by Grant H-1683 from the Welch Foundation (to J.I.).

*To whom correspondence should be addressed. Phone: 409-747-1403. Fax: 409-747-1404. E-mail: j.iwahara@utmb.edu.

[1]Abbreviations: NMR, nuclear magnetic resonance; HSQC, heteronuclear single-quantum coherence; TROSY, transverse relaxation optimized spectroscopy; RDC, residual dipolar coupling.

 Published on Web 08/19/2010

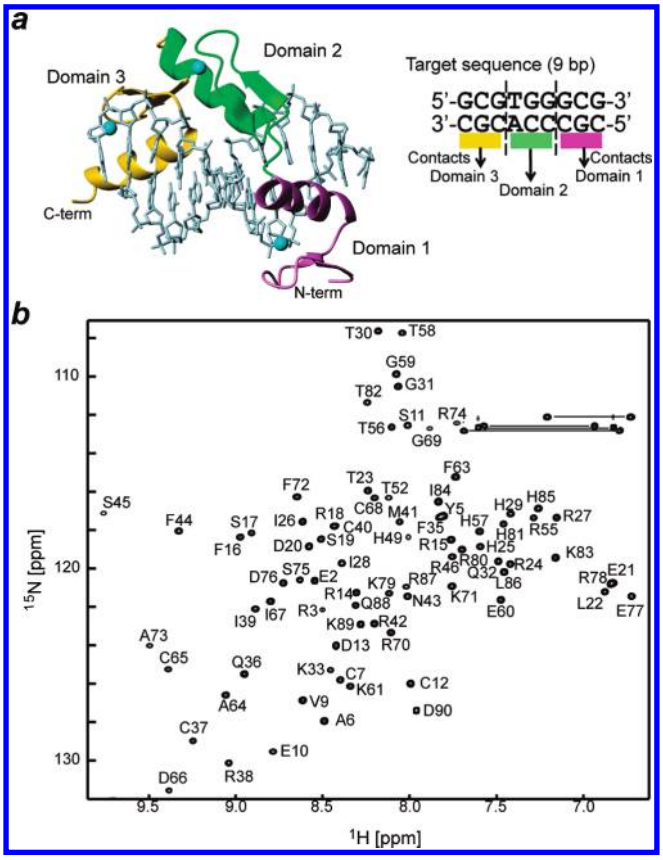

FIGURE 1: (a) The crystal structure of the Zif268 protein bound to DNA (PDB code 1AAY). Zif268 binds as a monomer via three Cys_2His_2-type zinc-finger domains (sphere, Zn^{2+} ions). Domains 1, 2, and 3 are colored in magenta, green, and yellow, respectively. The protein recognizes a 9-bp target sequence GCGTGGGCG. Each domain contacts three base pairs. (b) $^{1}H-^{15}N$ HSQC spectrum of the sequence-specific complex between the $^{13}C/^{15}N$-labeled Zif268 protein and unlabeled 12-bp DNA dAGCGTGGGCGTA/dTACGCCCACGCA, which contains the target site (underlined). Annotations are resonance assignments for backbone amide groups. Numbering of residues for the Zif268 protein is according to Pavletich and Pabo (*29*).

After disruption of the cells by sonication, the lysate was centrifuged at 40000*g*, and the supernatant was loaded onto a GSTPrep FF column (GE Healthcare). After the column was washed with 50 mM Tris-HCl (pH 7.5), 400 mM NaCl, and 1% Triton X-100, the GST-Zif268 fusion protein was eluted in 50 mM Tris, 400 mM NaCl, 10 mM glutathione, pH 7.5 (adjusted with HCl). The fusion protein was cleaved at 4 °C overnight with 100 units of HRV-3C protease (GE Healthcare). After the cleavage was confirmed by SDS−PAGE, the reaction mixture was concentrated to 5 mL with a Amicon Ultra-15 device (Millipore) and applied to a Sephacryl S100 26/60 column (GE Healthcare) equilibrated with a buffer of 50 mM Tris-HCl (pH7.5), 1000 mM NaCl, 2 mM glutathione, and 0.2 mM $ZnCl_2$ for separation by size-exclusion chromatography. Fractions containing the Zif268 protein were pooled, and the buffer was exchanged to 50 mM Tris-HCl (pH 7.0), 200 mM NaCl, 1 mM glutathione, 0.1 mM $ZnCl_2$, and 5% glycerol. The Zif268 protein was loaded onto a Mono-S 5/5 cation-exchange column (GE Healthcare) equilibrated with the same buffer and eluted with a NaCl gradient from 200 to 500 mM.

Preparation of DNA for NMR. Chemically synthesized oligonucleotides were purchased from either Midland Certified Reagents or Sigma Genosis. Each single-stranded DNA was purified by anion-exchange chromatography using a Mono-Q 10/100 column on an ÄKTA Purifier system (GE Healthcare). The NaCl gradient for the elution was typically 150−750 mM (optimal conditions depended on the lengths of oligonucleotides) in a buffer containing 50 mM Tris-HCl (pH 7.5) and 1 mM EDTA. Concentrations of the single-stranded DNA molecules were measured with UV absorbance at 260 nm and calculated with extinction coefficients estimated from the base compositions. After equimolar amounts of individual strands were mixed and annealed from 85 °C, the double-stranded DNA molecules were further purified by Mono-Q to remove the excess single-stranded DNA (*34*).

Resonance Assignment. All NMR experiments for $^{1}H/^{13}C/^{15}N$ resonance assignment were performed at 35 °C with either a Varian 800 MHz or 600 MHz spectrometer. Protein resonances for the complex between the Zif268 protein bound to 12-bp DNA were assigned using three-dimensional HN(CA)CO, HNCO, HNCA, HN(CO)CA, CBCA(CO)NH, C(CO)NH, H(CACO)NH, and ^{15}N-edited NOESY-HSQC spectra (*35*). The sample contained 1.0 mM $^{13}C/^{15}N$-labeled protein, 1.2 mM 12-bp DNA, 10 mM Tris-HCl (pH 6.8), 20 mM KCl, and 7% D_2O. The resonance assignments have been deposited to Biological Magnetic Resonance Bank (accession code 17130). Spectra were processed with the NMRPipe software (*36*) and analyzed with the NMRView program (*37*). Because the $^{1}H-^{15}N$ correlation spectra for complexes with longer DNA (24 and 30 bp) were similar to those for the complex with 12-bp DNA, their $^{1}H/^{15}N$ resonances were assigned based on the assignment of the 12-bp complex and ^{15}N-edited NOESY-HSQC measured for the individual complexes.

Structural Analysis. Residual dipolar coupling $^{1}D_{NH}$ induced by 10 mg/mL Pf1 phage (purchased from ASLA) was measured at 35 °C with the IPAP-HSQC method (*38*) for the Zif268 protein bound to 12-bp DNA. The best fitting of parameters representing the molecular alignment tensor against the 1.6 Å resolution crystal structure of the Zif268/DNA complex (PDB code 1AAY) was carried out using the Xplor-NIH software (*39*, *40*). Protein backbone torsion angles ϕ and ψ were predicted from $^{1}H_N$, $^{1}H_\alpha$, $^{13}C{=}O$, $^{13}C_\alpha$, $^{13}C_\beta$, and ^{15}N chemical shifts with the TALOS+ program (*41*).

NMR Real-Time Kinetics of Protein Translocation between Target DNA Molecules. Two solutions, I and II, were prepared in a buffer of 10 mM Tris-HCl (pH 7.2), 40 mM KCl, and 7% D_2O; solution I contained DNA 24A and the ^{15}N-labeled Zif268 protein (bound to DNA 24A), and solution II contained DNA 24B only. Kinetic experiments were initiated by mixing these solutions, which were immediately sealed into an NMR tube, and loaded onto a Varian 800 MHz NMR system. The process of translocation of the Zif268 protein from DNA 24A to DNA 24B was monitored at 30 °C using the COST-HSQC pulse sequence (*42*) with a repetition delay of 0.38 s. The protein concentration was 0.26 mM. The experiments was carried out at three different DNA concentrations: $([24A]_{total}, [24B]_{total})$ = (0.28, 0.24 mM), (0.44, 0.37 mM), and (0.61, 0.55 mM). The total protein concentration in the mixture was measured with the BCA protein assay kit (Pierce). The total DNA concentrations were measured by UV absorbance at 260 nm for solutions I and II as well as for their mixtures.

For the analysis of the NMR real-time kinetic data, populations of the Zif268 proteins bound to DNA 24A were calculated as $I_a/(I_a + I_b)$, in which I_a and I_b represents the intensities of HSQC signals from the proteins bound to DNA 24A and 24B, respectively. The population of the free protein is negligible

compared to that of the bound protein in the experiment, because DNA was in excess and its concentration (10^{-4}−10^{-3} M) is much higher than K_d (of a order of 10^{-9} M). Signals from four backbone amide groups that are well isolated for both complexes were used for the calculation of the populations. For each time point, the average for the four values for the different residues was used in the fitting calculation. The uncertainties in the obtained populations were estimated from the noise standard deviations of the spectra together with the standard error propagation method. Global fitting to the data sets at three different concentrations of DNA was performed via minimization of the following χ^2 function:

$$\chi^2 = \sum_h \left\{ \frac{(A_{1\mathrm{obs},h} - A_{1\mathrm{cal},h})^2}{\sigma_{1h}^2} \right\} + \sum_i \left\{ \frac{(A_{2\mathrm{obs},i} - A_{2\mathrm{cal},i})^2}{\sigma_{2i}^2} \right\} + \sum_j \left\{ \frac{(A_{3\mathrm{obs},j} - A_{3\mathrm{cal},j})^2}{\sigma_{3j}^2} \right\}$$

where A_1, A_2, and A_3 are populations of the proteins bound to DNA 24A for data sets 1, 2, and 3; annotations obs and cal stand for observed and calculated, respectively; indices h, i, and j are for individual time points; and σ represents uncertainty in an observed population. Concentrations [PD_A], [D_A], and [P] at time 0 were calculated from the total protein concentration, the total DNA concentrations, and K_d, whereas the other initial concentrations were [PD_B](0) = 0 and [D_B](0) = [D_B]$_{total}$ in this experiment. The time courses of the concentrations of individual components were calculated by the numerical integration of the rate equations (eqs 1−5, below) (*43*). Values of k_{off} and k_{DT} were optimized via the χ^2 minimization, in which A_{cal} values were calculated with the numerical integrations (*44*, *45*). Thus the fitting procedure does not require an analytical equation that represents time−course data. The uncertainty in the fitting parameters was estimated by using $\Delta\chi^2$ and a confidence limit of 68% (*46*). All calculations were carried out with Mathematica 7 (Wolfram).

Analysis of Context-Dependent Binding Preference. Using a Varian 800 MHz NMR system, two-dimensional ^{1}H−^{15}N TROSY and HSQC spectra were recorded at 35 °C for the ^{15}N-labeled Zif268 proteins bound to DNA duplexes shown in Figure 4. The NMR samples contained 0.3 mM protein and 0.9 mM DNA dissolved in a buffer of 10 mM Tris-HCl (pH 7.5), 20 mM KCl, and 7% D_2O. One-dimensional ^{1}H or ^{15}N slices containing only one signal were extracted with the NMRView software from the HSQC spectra for which the dimension for the line-shape analysis was processed with no window functions applied. Nonlinear least-squares fitting calculations to obtain apparent ^{1}H and ^{15}N transverse relaxation rates from the NMR line shapes were carried out by using an in-house C-program that makes use of the GNU Scientific Library. Populations of proteins bound to individual target sites were calculated from the signal intensities as well as the apparent ^{1}H and ^{15}N transverse relaxation rates by using eq 6. Errors in the calculated populations were estimated with standard error propagation based on the partial derivatives and the errors in involved parameters (*47*).

RESULTS

NMR of Zif268 Bound to the Target DNA. Sequence-specific complexes of the Zif268 protein with target DNA exhibited well-dispersed ^{1}H−^{15}N correlation spectra. We used three DNA duplexes of different length: 12 base pairs (bp), 24 bp, and 30 bp.

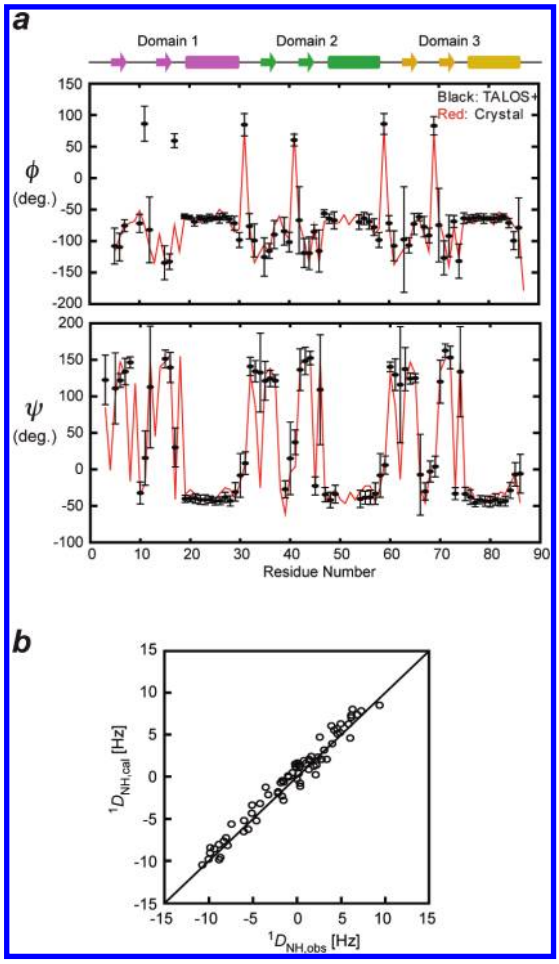

FIGURE 2: (a) Protein backbone torsion angles ϕ and ψ predicted by the TALOS+ program (*41*, *48*) from ^{1}H/^{13}C/^{15}N chemical shifts of the Zif268 protein bound to 12-bp DNA (dAGCGTGGGCGTA/dTACGCCCACGCA; target site underlined). Black points represent predicted angles. Each error bar corresponds to a standard deviation for the 10 best matches in the TALOS+ prediction. The torsion angles in the 1.6 Å resolution crystal structure (*30*) are shown in red. Secondary structures are indicated above the graphs. (b) Correlation between the measured and calculated residual dipolar coupling (RDC) $^1D_{NH}$ for the complex between the ^{2}H/^{15}N-labeled Zif268 protein and unlabeled 12-bp DNA.

Figure 1b shows an HSQC spectrum recorded for a specific complex between the ^{13}C/^{15}N-labeled Zif268 protein with unlabeled 12-bp DNA containing the 9-bp target sequence GCGTGGGCG. The backbone ^{1}HN, ^{15}N, ^{13}C═O, ^{13}Cα, and ^{13}Cβ resonances were assigned for 97% of residues. ^{1}H−^{15}N cross-peaks from Leu50 and Thr51 in the α-helix of domain 2 in the complex as well as the complexes with longer DNA (24 and 30 bp) were broadened beyond detection. One potential explanation for this resonance broadening is the exchange between free and bound states occurring in an intermediate exchange regime. However, the kinetic data shown in a later section clearly indicate that the dissociation of the complex occurs in a minute to hour time scale, and therefore, it is most likely that conformational exchange within the DNA-bound state causes the signal broadening. In fact, the crystal structure at 1.6 Å resolution (PDB code 1AAY) (*30*) shows two very different conformers for the side chain of Leu50 (one with χ_2 = 63°, the other with χ_2 = −83°).

Structural Information from Chemical Shifts and RDC. The backbone torsion angles ϕ and ψ were predicted from the

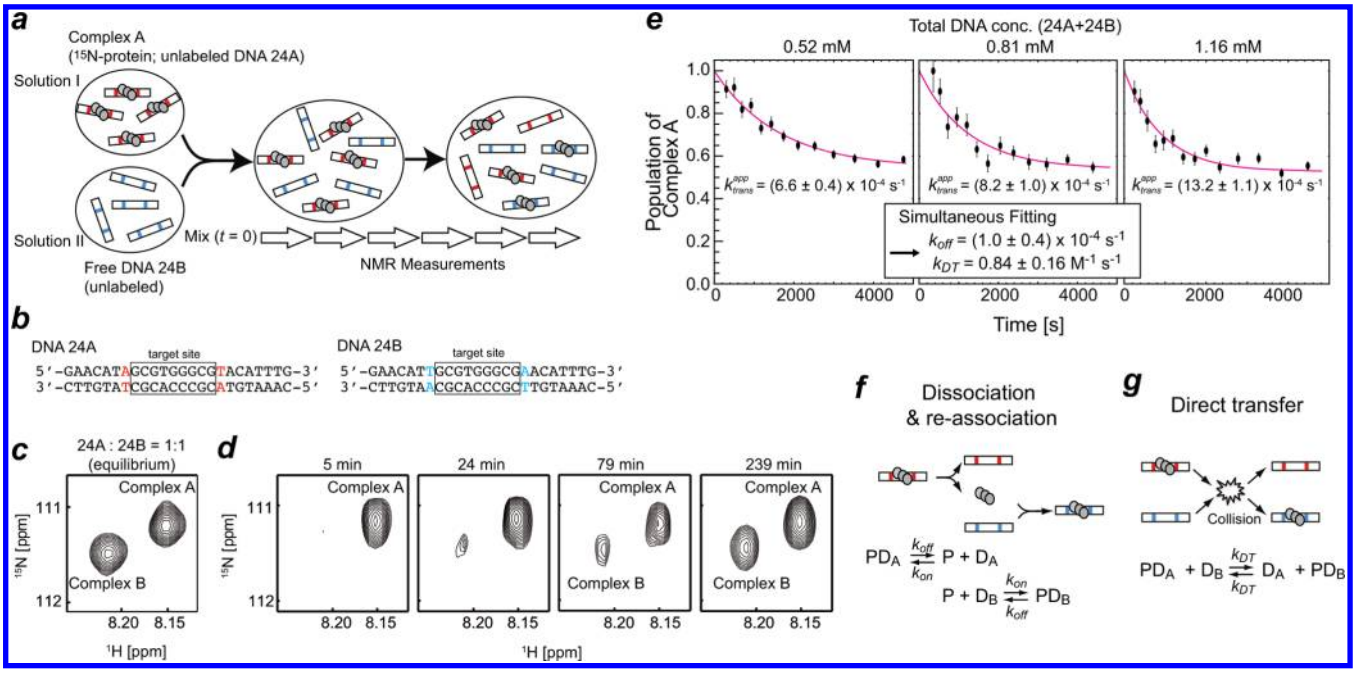

FIGURE 3: NMR-based real-time kinetics of translocation of the Zif268 protein between two target sites on different DNA molecules. (a) Schematic drawing of the experimental design. (b) The base sequences of DNA 24A and 24B. These sequences are identical except for two base pairs adjacent to the target sequence. (c) HSQC signals from Thr30 measured for a mixture containing 0.15 mM protein, 0.20 mM DNA 24A, and 0.20 mM DNA 24B. The intensities of the signals from the two complexes were found to be virtually the same for this mixture at equilibrium, indicating that the affinities of DNA 24A and 24B are the same. (d) Changes of the HSQC signals from Thr30 amide group upon mixing solutions I and II. The initial total concentrations of the protein and DNA duplexes 24A and 24B were 0.26, 0.28, and 0.24 mM, respectively. For the rapid data acquisition, the resolution of the ^{15}N dimension is lower for the spectra in panel d than the spectrum in panel c. (e) Real-time kinetics of protein translocation from DNA 24A to DNA 24B as monitored by NMR. Three experiments with different DNA concentrations were conducted (the total DNA concentrations are indicated on each graph). The values of the apparent pseudo-first-order rate constants for translocation (k_{trans}^{app}) obtained by fitting for individual data set are shown on each graph. The results of the global fitting are shown in a box. The curves shown in red together with data points were obtained with the global fitting calculation. (f, g) Two possible mechanisms for the intermolecular protein translocation between two DNA molecules.

^{1}H/^{13}C/^{15}N chemical shifts of the Zif268 protein/DNA complex by using the TALOS+ program (*41*, *48*). As shown in Figure 2a, the predicted ϕ and ψ angles are in a good agreement with those in the crystal structure of the specific complex. To obtain further information on the structure of the complex in solution, we also measured residual dipolar coupling (RDC) $^{1}D_{NH}$ induced by 10 mg/mL Pf1 phage for the ^{2}H-/^{15}N-labeled Zif268 protein bound to the 12-bp DNA. Using the obtained RDC data, the five parameters (i.e., magnitude, D_a; rhombicity, η; and three Euler angles) representing the molecular alignment tensor were fitted against the crystal structure. By this fitting procedure, D_a and η were determined to be −5.3 Hz and 0.54, respectively. As shown in Figure 2b, the experimental and calculated $^{1}D_{NH}$ data were in a good agreement, giving an RDC *R*-factor (*49*) of 0.136. These data suggest that the structure of Zif268 bound to the target DNA in solution is virtually identical to the crystal structure.

Kinetics of Protein Translocation between Target Sites on Different DNA Molecules. Using NMR, we analyzed the kinetics of the translocation process in which the Zif268 protein transfers from one target site to another. An initial attempt to analyze the process by using *z*-exchange spectroscopy (as we had successfully applied to the HoxD9 homeodomain (*3*, *4*, *7*)) was precluded due to very slow translocation of the Zif268 protein between the target sites. We then analyzed the translocation process by using a "real-time" approach based on NMR, which is schematically depicted in Figure 3a. In this approach, the complex between the Zif268 protein and a 24-bp DNA molecule (24A) is first prepared and mixed with a solution of another 24-bp DNA (24B). These DNA molecules, 24A and 24B, differ only in two base pairs adjacent to the target 9-bp sequence GCGTGGGCG (Figure 3b). When these two DNAs are bound to the Zif268 protein, we observed slightly different NMR chemical shifts for some protein residues due to the sequence differences between 24A and 24B. The relative affinities of these two DNA molecules appear to be virtually identical because the ratio of signal intensities for the proteins bound to DNA duplexes 24A and 24B was the same at equilibrium when equimolar concentrations of DNA duplexes were used (Figure 3c). In the present approach, we monitored translocation of the ^{15}N-labeled Zif268 protein from the target in DNA duplex 24A to another target in DNA duplex 24B using a series of HSQC spectra (examples shown in Figure 3d) recorded with the selective excitation method (*42*, *50*, *51*). This method permits the rapid acquisition of the two-dimensional spectra. Until the system reached equilibrium in 1−2 h, the signals from the protein bound to DNA duplex 24A became weaker, whereas those from the protein bound to 24B became stronger. The kinetic experiments were carried out with three different concentrations of DNA, and the time−course data obtained are shown in Figure 3e. Apparent pseudo-first-order rate constants for protein translocation between target DNA molecules (k_{trans}^{app}) were calculated individually for the three data sets using monoexponential fitting. k_{trans}^{app} was found to be larger at a higher concentration of DNA (Figure 3e).

As explained in previous studies (*4*, *5*, *7*, *52*−*56*), two mechanisms can contribute to the intermolecular protein translocation between two DNA molecules: (1) dissociation and reassociation (Figure 3f) and (2) direct transfer (Figure 3g). Assuming that the biochemical properties of DNA duplexes 24A

and 24B are virtually identical, the rate equations for translocation are given by

$$\frac{d}{dt}[PD_A] = -k_{off}[PD_A] + k_{on}[P][D_A] - k_{DT}[PD_A][D_B] + k_{DT}[PD_B][D_A] \quad (1)$$

$$\frac{d}{dt}[PD_B] = -k_{off}[PD_B] + k_{on}[P][D_B] - k_{DT}[PD_B][D_A] + k_{DT}[PD_A][D_B] \quad (2)$$

$$\frac{d}{dt}[D_A] = -k_{on}[P][D_A] + k_{off}[PD_A] - k_{DT}[PD_B][D_A] + k_{DT}[PD_A][D_B] \quad (3)$$

$$\frac{d}{dt}[D_B] = -k_{on}[P][D_B] + k_{off}[PD_B] - k_{DT}[PD_A][D_B] + k_{DT}[PD_B][D_A] \quad (4)$$

$$\frac{d}{dt}[P] = -k_{on}[P][D_A] - k_{on}[P][D_B] + k_{off}[PD_A] + k_{off}[PD_B] \quad (5)$$

in which [D], [P], and [PD] represent the concentrations of free DNA, free protein, and complexes, respectively; k_{off}, the dissociation rate constant; k_{on}, the association rate constant; and k_{DT}, the second-order rate constant for direct transfer between the two specific sites on different DNA molecules. If $[D] \gg K_d$ (this is satisfied in the present experiment), $k_{on}[D]$ is much greater than k_{off}, and therefore, the rate-limiting step for protein translocation via the dissociation and reassociation mechanism is the dissociation, a first-order event. So, if this mechanism is predominant, the translocation rate should be virtually independent of the free DNA concentration. On the other hand, the translocation via direct transfer is a second-order reaction, and therefore its rate depends on the free DNA concentration. Thus, our experimental data showing the DNA concentration dependence of k_{trans}^{app} suggest the presence of the direct transfer mechanism.

Using eqs 1−5, k_{off} and k_{DT} were determined by simultaneous best fitting against the experimental data at three different DNA concentrations. The k_{on} rate constant cannot be determined by this experiment because the association is much faster than the dissociation and direct transfer processes that limit the overall kinetics of translocation. Although the k_{on} and k_{off} rate constants were restrained by some different values of the dissociation constant $K_d = k_{off}/k_{on}$ in the previously known range (10^{-10}−10^{-8} M) (*24*), the determined values of k_{off} and k_{DT} rate constants were unaffected by the variation of K_d. The dissociation rate constant k_{off} was determined to be $(1.0 \pm 0.4) \times 10^{-4}$ s^{-1} at 40 mM KCl. This is consistent with k_{off} measured at a higher ionic strength using surface plasmon resonance (2×10^{-4} s^{-1} at 90 mM KCl) (*20*). The second-order rate constant k_{DT} for the direct transfer between the target DNA duplexes was determined to be 0.84 ± 0.16 M^{-1} s^{-1}. Under the current experimental conditions with 0.3−0.9 mM free DNA, the direct transfer accounts for 70−90% of the translocation of Zif268 between the two target sites.

Translocation between Two Sites on the Same DNA Molecule. If there are two target sites on the same DNA molecules, it is possible for the Zif268 protein to transfer more quickly between the target sites via sliding on DNA. To pursue this possibility, we designed 30-bp DNA molecules 30$\vec{A}\vec{B}$, 30$\vec{B}\vec{A}$, and 30$\vec{B}\vec{A}$ (Figure 4a), in which there are two target sites separated by 5 bp, and analyzed their interactions with the Zif268 protein. The two sites, A and B, in these duplexes correspond to those in DNA molecules 24A and 24B, respectively. We recorded two-dimensional ^{1}H−^{15}N correlation NMR spectra at 800 MHz for the Zif268 protein bound to either of two target sites on the same DNA molecule (Figure 4a). In the experiment, we used a total molar concentration of the target sites that was 6-fold higher than that of the Zif268 protein, such that the vast majority of complexes should contain a single protein molecule bound to either of the two target sites on a DNA duplex (although the duplexes could accommodate two proteins). As seen in the experiments with DNA 24A and 24B, some residues of Zif268 exhibited two separate signals from the proteins bound to A and B. This indicates that translocation of the Zif268 protein between the two target sites occurs in the slow exchange regime. By using a different set of DNA duplexes for which one of the two target sites is disrupted by base substitutions (Figure 4b), we were able to individually assign signals from the proteins at sites A and B for DNA duplexes 30$\vec{A}\vec{B}$, 30$\vec{B}\vec{A}$, and 30$\vec{B}\vec{A}$.

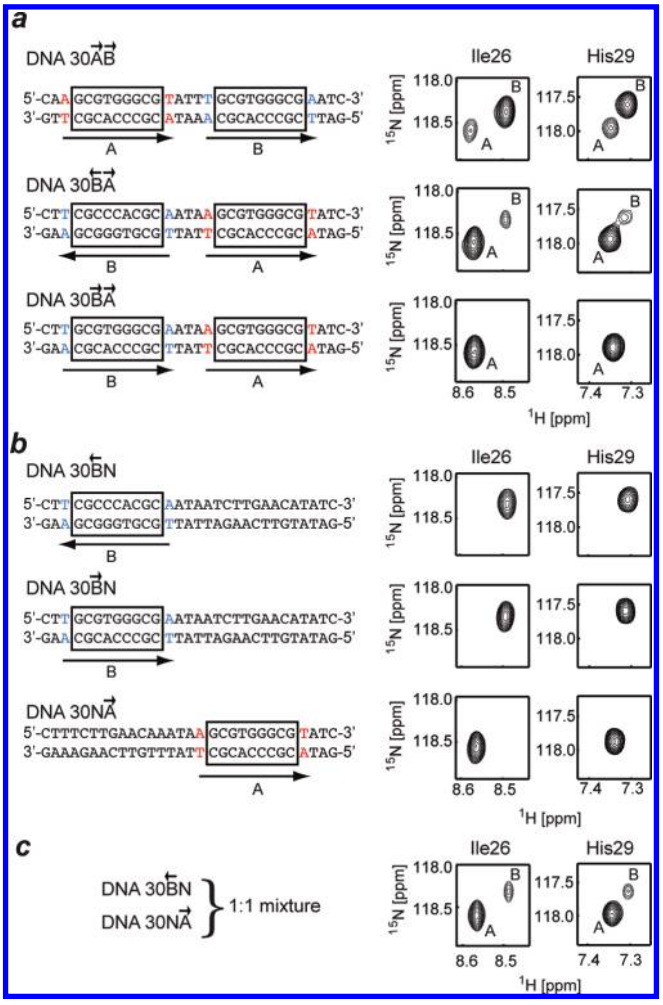

FIGURE 4: (a) TROSY signals measured for the ^{15}N-labeled Zif268 proteins bound to a 30-bp DNA containing two target sites, A and B, that correspond to those in DNA 24A and 24B, respectively. Signals for residue Ile26 and His29 are shown. Note that the intensities of the signals from the Zif268 proteins at sites A and B are significantly different. The NMR samples contained 0.3 mM protein and 0.9 mM DNA (b) TROSY signals measured for the ^{15}N-labeled Zif268 proteins bound to a 30-bp DNA containing only one target site. The signals shown in panel a were assigned using these spectra. (c) TROSY signals observed for the mixture of 0.2 mM ^{15}N-labeled protein, 0.32 mM DNA 30$\vec{B}\vec{A}$, and 0.32 mM DNA 30$\vec{B}\vec{A}$. For all panels, the NMR spectra were recorded at 35 °C, and the buffer conditions were 10 mM Tris-HCl (pH 7.5), 20 mM KCl, and 7% D_2O.

Table 1: Relative Populations of the Zif268 Protein at Sites A and B on DNA Molecules 30$\vec{A}\vec{B}$ and 30$\vec{B}\vec{A}$ Determined by NMR[a]

DNA	protein amide[b]	binding site	$R_{2,H}^{app}$ (s^{-1})[c]	$R_{2,N}^{app}$ (s^{-1})[d]	relative intensity[e]	relative population[f]
30$\vec{A}\vec{B}$	I26	A	103.8 ± 3.1	58.4 ± 1.9	0.255 ± 0.003	0.371 ± 0.018
		B	88.8 ± 1.0	45.5 ± 0.5	0.745 ± 0.003	0.629 ± 0.018
	H29	A	92.9 ± 2.5	47.6 ± 1.3	0.286 ± 0.003	0.343 ± 0.015
		B	83.3 ± 0.8	44.6 ± 0.5	0.714 ± 0.003	0.657 ± 0.015
	T30	A	101.9 ± 2.5	45.3 ± 1.3	0.289 ± 0.003	0.399 ± 0.016
		B	81.6 ± 0.9	41.9 ± 0.5	0.711 ± 0.003	0.601 ± 0.016
						overall A: 0.371 ± 0.014
						overall B: 0.629 ± 0.014
30$\vec{B}\vec{A}$	I26	A	85.5 ± 2.2	53.3 ± 1.5	0.792 ± 0.004	0.733 ± 0.043
		B	111.7 ± 9.5	44.4 ± 4.2	0.208 ± 0.004	0.267 ± 0.043
	H29	A	90.7 ± 1.6	42.4 ± 1.2	0.779 ± 0.004	0.729 ± 0.034
		B	92.4 ± 6.4	53.7 ± 4.4	0.221 ± 0.004	0.271 ± 0.034
	T30	A	91.9 ± 1.7	40.2 ± 0.9	0.794 ± 0.004	0.830 ± 0.026
		B	81.8 ± 5.8	39.1 ± 4.1	0.206 ± 0.004	0.170 ± 0.026
						overall A: 0.764 ± 0.035
						overall B: 0.236 ± 0.035

[a] $^1H-^{15}N$ HSQC spectra recorded on the ^{15}N-labeled Zif268 protein bound to an unlabeled 30-bp DNA molecule containing two target sites, A and B, were used. [b] Backbone amide that showed isolated ^1H and ^{15}N resonances for both sites A and B. [c] Apparent ^1H transverse relaxation rates. [d] Apparent ^{15}N transverse relaxation rates. [e] Given by $I_A/(I_A + I_B)$ and $I_B/(I_A + I_B)$ for sites A and B, respectively, where I represents a peak height. Errors are based on noise standard deviations of the spectra. These correspond to populations estimated with no relaxation effects taken into consideration. [f] Populations calculated with eq 6. The value of τ used was 9.2 ms.

We carried out the *z*-exchange experiments for the kinetic analysis of the translocation between the two target sites on the 30-bp DNA. In this case, both intermolecular transfer and sliding can occur for the translocation of the proteins between the two sites on the DNA molecules. As shown in the previous subsection, the intermolecular transfer between different DNA molecules should occur on a minute to hour time scale. If sliding is as fast as 0.5−50 s^{-1}, exchange cross-peaks should appear in the *z*-exchange experiment (*4*, *7*, *57*, *58*). However, no exchange cross-peaks were observed in the *z*-exchange experiments for these samples with DNA containing two target sites at 40 mM KCl and 300 mM KCl (data not shown), which indicates that transfer of the Zif268 protein from a target site to the other via sliding is also slower than in the order of a second.

Populations of Proteins Bound to Different Target Sites. Interestingly, the peak intensities of signals from proteins bound to sites A and B in the 30-bp DNA molecules were found to differ substantially (Figure 4a). The intensities of signals from the protein at site B of DNA 30$\vec{A}\vec{B}$, for example, were significantly higher than the intensities of corresponding signals from the protein at site A. On the contrary, signals from the protein at site B were weaker than those from the protein at site A in DNA 30$\vec{B}\vec{A}$ and 30$\vec{B}\vec{A}$ (Figure 4a); in fact, the signals from the protein at site B of DNA 30$\vec{B}\vec{A}$ were too weak to be observed. As mentioned above, two complexes with sites A and B exhibited the same signal intensities at equilibrium with a 1:1 mixture of the 24-bp DNA duplexes 24A and 24B, in which the nucleotides surrounding the target sites are identical (Figure 3c). These data suggest that the populations of the proteins at target sites A and B are dependent on their locations and orientations.

The quantitative determination of populations from NMR data requires information about ^1H and ^{15}N relaxations that are relevant to intensities of the signals. It is likely that the ^1H longitudinal relaxation rates for proteins at sites A and B are almost identical because the $^1H-^1H$ dipolar interaction network should be virtually identical for the two states. However, the transverse relaxation rates can be quite different for the proteins at sites A and B, if a conformational exchange is present to a different degree. Provided that the NMR line shapes are Lorentzian in both ^1H and ^{15}N dimensions, the ratio of the peak height I_B to I_A is given by

$$\frac{I_B}{I_A} = \frac{p_B}{p_A} \frac{R_{2,H}^A R_{2,N}^A}{R_{2,H}^B R_{2,N}^B} \frac{\exp(-R_{2,H}^B \tau)}{\exp(-R_{2,H}^A \tau)} \quad (6)$$

where R_2 represents an apparent transverse relaxation rate and τ represents an overall time for $^1H-^{15}N$ coherence transfer in the $^1H-^{15}N$ correlation experiment. For the population analysis, we used the HSQC data rather than TROSY because theoretical consideration suggests that NMR line shapes for HSQC processed with no window function can be better represented by the Lorentzian shapes than those for TROSY. The apparent ^1H and ^{15}N transverse relaxation rates were calculated by line-shape fitting against one-dimensional slices of HSQC spectra. Using eq 6, the populations of proteins bound to sites A and B were calculated from the relaxation rates and signal intensities for backbone amide groups of Ile26, His29, and Thr30, which exhibited resonances isolated in both ^1H and ^{15}N dimensions for the two sites.

Table 1 shows the data for the calculations of populations of proteins at the two target sites on DNA duplexes 30$\vec{A}\vec{B}$ and 30$\vec{B}\vec{A}$. It was found that 37% of the Zif268 protein is at site A and 63% at site B on DNA 30$\vec{A}\vec{B}$, whereas the populations of the proteins at sites A and B on DNA 30$\vec{B}\vec{A}$ are 76% and 24%, respectively. It is likely that the populations of the sites A and B in DNA 30$\vec{B}\vec{A}$ differ to a greater degree as the signals from the protein bound to the site B are too weak to be observed. These data indicate that the binding affinity of a target site depends on the context in which the sequence is located in DNA.

To investigate a possibility that two specific sites in the same DNA somehow affect each other in the process of Zif268 binding, we carried out an additional similar experiment in which a 1:1 mixture of two 30-bp DNA duplexes containing only one target site at different locations (i.e., 30$\vec{B}$N and 30N$\vec{A}$) was used instead. As shown in Figure 4c, the ratio of the signal intensities for the Zif268 proteins bound to sites A and B for the mixture was found to be similar to those for DNA 30$\vec{B}\vec{A}$. This result clearly indicates that the binding preference is not due to the interaction between the target sites.

DISCUSSION

Direct Transfer of the Zif268 Protein between Its Target Sites. Although the direct transfer mechanism for translocation between DNA molecules was found almost 3 decades ago (*52*, *54*), there are only a few reports on the experimental determinations of the kinetic rate constants for direct transfers of proteins (*4*, *5*, *8*). For the HoxD9 (*4*) and Oct-1 (*8*) proteins, direct transfer between their target DNA molecules occurs with the second-order rate constants (k_{DT}) of 6×10^4 M^{-1} s^{-1} and 3×10^4 M^{-1} s^{-1}, respectively. Surprisingly, the obtained value of k_{DT} for Zif268 (0.84 ± 0.16 M^{-1} s^{-1}) indicates that direct transfer of the Zif268 protein between its target DNA sites is >30000-fold slower than corresponding direct transfers of the HoxD9 homeodomain and the Oct-1 protein under similar conditions. This discrepancy is very intriguing because the affinities of these three proteins to their target DNA sites are comparable (*3*, *24*, *59*). As discussed previously (*4*, *60*), the highly efficient direct transfer for the homeodomain may arise from the dynamics of the N-terminal tail that could locally dissociate from DNA and capture another DNA molecule, thereby allowing the protein molecule to form a transient structure bridging two DNA molecules. However, there is no corresponding tail in Zif268. Local dissociation of zinc-finger domains in the specific complex of Zif268 is likely to be inefficient, because each zinc-finger domain forms 7−8 hydrogen bonds with DNA (3−4 bonds are with bases) in the specific complex (*29*). These aspects of HoxD9 and Zif268 could be responsible for their very different k_{DT} values.

Judging from the value determined for k_{DT} and the low natural abundance of the 9-bp target sequence, it is unlikely that direct transfer between the target sites is important for Zif268 in cells. Interestingly, however, direct transfer of Zif268 between nonspecific DNA molecules was found to be extremely fast with k_{DT} on the order of 10^7 M^{-1} s^{-1} (data not shown). The high efficiency for direct transfer between nonspecific DNA sites might be due to the interdomain dynamics that could allow the Zif268 protein to transiently bridge two DNA molecules using different domains. Since the protein−DNA interactions are weaker for nonspecific DNA, the three zinc-finger domains of Zif268 may be far more dynamic in a nonspecific complex than in a specific complex. Our results suggest that once it finds a target site, the Zif268 protein stays there for a long time (with a half-life time of ~2 h at 40 mM KCl), although this protein can transfer very quickly between nonspecific DNA via direct transfer during the target search process.

Context-Dependent Binding Preference. Our NMR data on sequence-specific interactions between the Zif268 protein and its target sites suggest that the relative affinities of the target sites depend on their locations and orientations on DNA. The context-dependent binding preference may be caused by subtle structural differences due to different sequences adjacent to the target sequence and/or long-range electrostatic interactions. The non-uniform affinities for the same target sequence could be important for the functions of the transcription factor. A recent study of genome-wide *in vivo* Zif268 binding sites in monocytic differentiation by means of chromatin immunoprecipitation with a promoter array (ChIP-on-chip) showed that Zif268 shows relative enrichments of 5−50-fold at promoter regions for different target genes (*61*). While the variation of *in vivo* Zif268 occupancies can reflect influences of other proteins bound to DNA, it should be noted that the context-dependent binding preference found in our present study could also contribute to the variation at this level. The context dependence might be of biological significance for fine-tuning of populations of the transcription factor at its functionally important sites.

ACKNOWLEDGMENT

The NMR facilities of the UTMB Sealy Center for Structural Biology and Molecular Biophysics were supported in part by the Sealy and Smith Foundation, the W. M. Keck Foundation, and the John S. Dunn Foundation. We thank Dr. Tianzhi Wang for technical support and maintenance of the NMR instruments.

REFERENCES

1. Härd, T. (1999) NMR studies of protein-nucleic acid complexes: structures, solvation, dynamics and coupled protein folding. *Q. Rev. Biophys. 32*, 57–98.
2. Bonvin, A. M., Boelens, R., and Kaptein, R. (2005) NMR analysis of protein interactions. *Curr. Opin. Chem. Biol. 9*, 501–508.
3. Iwahara, J., and Clore, G. M. (2006) Detecting transient intermediates in macromolecular binding by paramagnetic NMR. *Nature 440*, 1227–1230.
4. Iwahara, J., and Clore, G. M. (2006) Direct observation of enhanced translocation of a homeodomain between DNA cognate sites by NMR exchange spectroscopy. *J. Am. Chem. Soc. 128*, 404–405.
5. Iwahara, J., Zweckstetter, M., and Clore, G. M. (2006) NMR structural and kinetic characterization of a homeodomain diffusing and hopping on nonspecific DNA. *Proc. Natl. Acad. Sci. U.S.A. 103*, 15062–15067.
6. Iwahara, J., Schwieters, C. D., and Clore, G. M. (2004) Characterization of nonspecific protein-DNA interactions by ^{1}H paramagnetic relaxation enhancement. *J. Am. Chem. Soc. 126*, 12800–12808.
7. Sahu, D., Clore, G. M., and Iwahara, J. (2007) TROSY-based z-exchange spectroscopy: application to the determination of the activation energy for intermolecular protein translocation between specific sites on different DNA molecules. *J. Am. Chem. Soc. 129*, 13232–13237.
8. Doucleff, M., and Clore, G. M. (2008) Global jumping and domain-specific intersegment transfer between DNA cognate sites of the multidomain transcription factor Oct-1. *Proc. Natl. Acad. Sci. U.S.A. 105*, 13871–13876.
9. Clore, G. M., and Iwahara, J. (2009) Theory, practice, and applications of paramagnetic relaxation enhancement for the characterization of transient low-population states of biological macromolecules and their complexes. *Chem. Rev. 109*, 4108–4139.
10. Baumgartel, K., Genoux, D., Welzl, H., Tweedie-Cullen, R. Y., Koshibu, K., Livingstone-Zatchej, M., Mamie, C., and Mansuy, I. M. (2008) Control of the establishment of aversive memory by calcineurin and Zif268. *Nat. Neurosci. 11*, 572–578.
11. Beckmann, A. M., and Wilce, P. A. (1997) Egr transcription factors in the nervous system. *Neurochem. Int. 31*, 477–510discussion 517−476.
12. Bozon, B., Davis, S., and Laroche, S. (2003) A requirement for the immediate early gene zif268 in reconsolidation of recognition memory after retrieval. *Neuron 40*, 695–701.
13. Hall, J., Thomas, K. L., and Everitt, B. J. (2001) Cellular imaging of zif268 expression in the hippocampus and amygdala during contextual and cued fear memory retrieval: selective activation of hippocampal CA1 neurons during the recall of contextual memories. *J. Neurosci. 21*, 2186–2193.
14. Jones, M. W., Errington, M. L., French, P. J., Fine, A., Bliss, T. V., Garel, S., Charnay, P., Bozon, B., Laroche, S., and Davis, S. (2001) A requirement for the immediate early gene Zif268 in the expression of late LTP and long-term memories. *Nat. Neurosci. 4*, 289–296.
15. Mokin, M., and Keifer, J. (2005) Expression of the immediate-early gene-encoded protein Egr-1 (zif268) during in vitro classical conditioning. *Learn. Mem. 12*, 144–149.
16. Wolfe, S. A., Nekludova, L., and Pabo, C. O. (2000) DNA recognition by Cys_2His_2 zinc finger proteins. *Annu. Rev. Biophys. Biomol. Struct. 29*, 183–212.
17. Beerli, R. R., Segal, D. J., Dreier, B., and Barbas, C. F., 3rd (1998) Toward controlling gene expression at will: specific regulation of the erbB-2/HER-2 promoter by using polydactyl zinc finger proteins constructed from modular building blocks. *Proc. Natl. Acad. Sci. U.S.A. 95*, 14628–14633.
18. Wu, H., Yang, W. P., and Barbas, C. F., III (1995) Building zinc fingers by selection: toward a therapeutic application. *Proc. Natl. Acad. Sci. U.S.A. 92*, 344–348.

19. Christy, B., and Nathans, D. (1989) DNA binding site of the growth factor-inducible protein Zif268. *Proc. Natl. Acad. Sci. U.S.A. 86*, 8737–8741.
20. Yang, W. P., Wu, H., and Barbas, C. F., III (1995) Surface plasmon resonance based kinetic studies of zinc finger-DNA interactions. *J. Immunol. Methods 183*, 175–182.
21. Turk, J. A., and Smithrud, D. B. (2003) Synthesis and evaluation of peptidomimetics that bind DNA. *Bioorg. Med. Chem. 11*, 2355–2365.
22. Elrod-Erickson, M., and Pabo, C. O. (1999) Binding studies with mutants of Zif268. Contribution of individual side chains to binding affinity and specificity in the Zif268 zinc finger-DNA complex. *J. Biol. Chem. 274*, 19281–19285.
23. Greisman, H. A., and Pabo, C. O. (1997) A general strategy for selecting high-affinity zinc finger proteins for diverse DNA target sites. *Science 275*, 657–661.
24. Hamilton, T. B., Borel, F., and Romaniuk, P. J. (1998) Comparison of the DNA binding characteristics of the related zinc finger proteins WT1 and EGR1. *Biochemistry 37*, 2051–2058.
25. Rebar, E. J., and Pabo, C. O. (1994) Zinc finger phage: affinity selection of fingers with new DNA-binding specificities. *Science 263*, 671–673.
26. Shi, Y., and Berg, J. M. (1995) A direct comparison of the properties of natural and designed zinc-finger proteins. *Chem. Biol. 2*, 83–89.
27. Swirnoff, A. H., and Milbrandt, J. (1995) DNA-binding specificity of NGFI-A and related zinc finger transcription factors. *Mol. Cell. Biol. 15*, 2275–2287.
28. Elrod-Erickson, M., Benson, T. E., and Pabo, C. O. (1998) High-resolution structures of variant Zif268-DNA complexes: implications for understanding zinc finger-DNA recognition. *Structure 6*, 451–464.
29. Pavletich, N. P., and Pabo, C. O. (1991) Zinc finger-DNA recognition: crystal structure of a Zif268-DNA complex at 2.1 Å. *Science 252*, 809–817.
30. Elrod-Erickson, M., Rould, M. A., Nekludova, L., and Pabo, C. O. (1996) Zif268 protein-DNA complex refined at 1.6 Å: a model system for understanding zinc finger-DNA interactions. *Structure 4*, 1171–1180.
31. Kim, C. A., and Berg, J. M. (1996) A 2.2 Å resolution crystal structure of a designed zinc finger protein bound to DNA. *Nat. Struct. Biol. 3*, 940–945.
32. Wolfe, S. A., Grant, R. A., Elrod-Erickson, M., and Pabo, C. O. (2001) Beyond the "recognition code": structures of two Cys_2His_2 zinc finger/TATA box complexes. *Structure 9*, 717–723.
33. Wolfe, S. A., Greisman, H. A., Ramm, E. I., and Pabo, C. O. (1999) Analysis of zinc fingers optimized via phage display: evaluating the utility of a recognition code. *J. Mol. Biol. 285*, 1917–1934.
34. Iwahara, J., Wojciak, J. M., and Clubb, R. T. (2001) Improved NMR spectra of a protein-DNA complex through rational mutagenesis and the application of a sensitivity optimized isotope-filtered NOESY experiment. *J. Biomol. NMR 19*, 231–241.
35. Cavanagh, J., Fairbrother, W. J., Palmer, A. G., III, Rance, M., and Skelton, N. J. (2007) Protein NMR Sprectroscopy: Principles and Practice, 2nd ed., Elsevier Academic Press, Burlington, MA.
36. Delaglio, F., Grzesiek, S., Vuister, G. W., Zhu, G., Pfeifer, J., and Bax, A. (1995) NMRPipe—a multidimensional spectral processing system based on Unix pipes. *J. Biomol. NMR 6*, 277–293.
37. Johnson, B. A., and Blevins, R. A. (1994) NMRView—a computer-program for the visualization and analysis of NMR data. *J. Biomol. NMR 4*, 603–614.
38. Ottiger, M., Delaglio, F., and Bax, A. (1998) Measurement of J and dipolar couplings from simplified two-dimensional NMR spectra. *J. Magn. Reson. 131*, 373–378.
39. Schwieters, C. D., Kuszewski, J. J., and Clore, G. M. (2006) Using Xplor-NIH for NMR molecular structure determination. *Prog. NMR Spectrosc. 48*, 47–62.
40. Schwieters, C. D., Kuszewski, J. J., Tjandra, N., and Clore, G. M. (2003) The Xplor-NIH NMR molecular structure determination package. *J. Magn. Reson. 160*, 65–73.
41. Shen, Y., Delaglio, F., Cornilescu, G., and Bax, A. (2009) TALOS+: a hybrid method for predicting protein backbone torsion angles from NMR chemical shifts. *J. Biomol. NMR 44*, 213–223.
42. Deschamps, M., and Campbell, I. D. (2006) Cooling overall spin temperature: protein NMR experiments optimized for longitudinal relaxation effects. *J. Magn. Reson. 178*, 206–211.
43. Heirer, E., Norsett, S. P., and Wanner, G. (1991) Solving Ordinary Differential Equations I: Nonstiff Problems, Springer, Berlin.
44. Brewer, D., Barenco, M., Callard, R., Hubank, M., and Stark, J. (2008) Fitting ordinary differential equations to short time course data. *Philos. Trans. R. Soc. London, Ser. A 366*, 519–544.
45. Tjoa, I. B., and Biegler, L. T. (1991) Simultaneous solution and optimization strategies for parameter-estimation of differential-algebraic equation systems. *Ind. Eng. Chem. Res. 30*, 376–385.
46. Press, W. H., Teukolsky, S. A., Vetterling, W. T., and Flannery, B. P. (2007) Numerical Recipies: The Art of Scientific Computing, 3rd ed., Cambridge University Press, New York.
47. Bevington, P. R., and Robinson, D. K. (2003) Data Reduction and Error Analysis, 3rd ed., McGraw-Hill, Boston, MA.
48. Cornilescu, G., Delaglio, F., and Bax, A. (1999) Protein backbone angle restraints from searching a database for chemical shift and sequence homology. *J. Biomol. NMR 13*, 289–302.
49. Clore, G. M., and Garrett, D. S. (1999) R-factor, free R, and complete cross-validation for dipolar coupling refinement of NMR structures. *J. Am. Chem. Soc. 121*, 9008–9012.
50. Pervushin, K., Vogeli, B., and Eletsky, A. (2002) Longitudinal ^1H relaxation optimization in TROSY NMR spectroscopy. *J. Am. Chem. Soc. 124*, 12898–12902.
51. Schanda, P., and Brutscher, B. (2005) Very fast two-dimensional NMR spectroscopy for real-time investigation of dynamic events in proteins on the time scale of seconds. *J. Am. Chem. Soc. 127*, 8014–8015.
52. Berg, O. G., Winter, R. B., and von Hippel, P. H. (1981) Diffusion-driven mechanisms of protein translocation on nucleic acids. 1. Models and theory. *Biochemistry 20*, 6929–6948.
53. Cho, S., and Wensink, P. C. (1997) DNA binding by the male and female doublesex proteins of *Drosophila melanogaster*. *J. Biol. Chem. 272*, 3185–3189.
54. Fried, M. G., and Crothers, D. M. (1984) Kinetics and mechanism in the reaction of gene regulatory proteins with DNA. *J. Mol. Biol. 172*, 263–282.
55. Lieberman, B. A., and Nordeen, S. K. (1997) DNA intersegment transfer, how steroid receptors search for a target site. *J. Biol. Chem. 272*, 1061–1068.
56. Ruusala, T., and Crothers, D. M. (1992) Sliding and intermolecular transfer of the lac repressor: kinetic perturbation of a reaction intermediate by a distant DNA sequence. *Proc. Natl. Acad. Sci. U.S.A. 89*, 4903–4907.
57. Farrow, N. A., Zhang, O., Forman-Kay, J. D., and Kay, L. E. (1994) A heteronuclear correlation experiment for simultaneous determination of ^{15}N longitudinal decay and chemical exchange rates of systems in slow equilibrium. *J. Biomol. NMR 4*, 727–734.
58. Li, Y., and Palmer, A. G., 3rd (2009) TROSY-selected ZZ-exchange experiment for characterizing slow chemical exchange in large proteins. *J. Biomol. NMR 45*, 357–360.
59. Kristie, T. M., and Sharp, P. A. (1990) Interactions of the Oct-1 POU subdomains with specific DNA sequences and with the HSV alpha-trans-activator protein. *Genes Dev. 4*, 2383–2396.
60. Vuzman, D., Azia, A., and Levy, Y. Searching DNA via a "Monkey Bar" mechanism: the significance of disordered tails, *J. Mol. Biol.* 396, 674-684.
61. Kubosaki, A., Tomaru, Y., Tagami, M., Arner, E., Miura, H., Suzuki, T., Suzuki, M., Suzuki, H., and Hayashizaki, Y. (2009) Genome-wide investigation of in vivo EGR-1 binding sites in monocytic differentiation. *Genome Biol. 10*, R41.